Monitoring the Intragastric Distribution of a Colloidal Drug Carrier Model by Magnetic Resonance Imaging

Henryk Faas,[1] Werner Schwizer,[2] Christine Feinle,[2] Hans Lengsfeld,[3] Chris de Smidt,[3] Peter Boesiger,[1] Michael Fried,[2] and Thomas Rades[3,4]

Received September 14, 2000; accepted January 12, 2001

Purpose. Monitoring the distribution of drugs or drug delivery systems in the human gastrointestinal tract is an important prerequisite for the design of orally administered drugs. We investigated the intragastric distribution of a colloidal drug delivery system (liposomes containing the contrast agent Gd-DOTA) by magnetic resonance imaging.

Methods. Following ingestion of a liquid or a solid meal, gastric distribution of liposomes released from a capsule and the fat component of the solid meal were tracked in 7 healthy subjects for 90 min. Liposomes were identified in gastric content by the increased signal intensity provided by the encapsulated Gd-DOTA.

Results. With the liquid meal, liposomes initially formed a layer on the surface before distributing in 86 ± 2% of gastric content (maximum distribution volume) within 42 ± 6 min. With the solid meal, maximum distribution (7 ± 1%, reached within 24 ± 6 min) was confined to a small volume in the fundus without forming a layer, suggesting that distribution was related to the accessible liquid compartment. Fat distribution was inhomogeneous and concentrated in the fundus.

Conclusions. Intragastric distribution of a colloidal drug carrier model, such as Gd-DOTA-filled liposomes, varies between meals of different composition. These differences can be monitored in three dimensions in humans by MRI.

KEY WORDS: intragastric drug distribution; colloidal system; liposomes; solid meal; liquid meal; magnetic resonance imaging.

INTRODUCTION

Monitoring the distribution of drugs or formulations in the human gastrointestinal tract is of great interest in the development of oral drug delivery systems. It is particularly important for drugs that act locally in the gastrointestinal tract (1), if site specific absorption is desired (2), in case of drug-food interactions (3) or in conditions in which release of the drug close to the site of macronutrient digestion is required, as is the case in pancreatic insufficiency and cystic fibrosis (4). Furthermore, *in vivo* monitoring of dosage forms would allow establishing optimal drug delivery based on data on local release in the gastrointestinal tract.

In humans, gamma scintigraphy has been used successfully to investigate the *in vivo* fate of pharmaceutical dosage forms (5–7). Recently, magnetic resonance imaging (MRI) has been proposed as an alternative or additional tool to gamma scintigraphy to study drug distribution in the gastrointestinal tract (8). The technique offers the possibility to acquire three-dimensional information on the distribution of drug delivery systems together with visualization of the anatomical structures in vicinity of the delivery system.

MRI is a noninvasive technique free of ionizing radiation, based on the principle of nuclear magnetic resonance (NMR). In NMR, protons in a strong, static magnetic field emit a NMR signal in response to electromagnetic irradiation at radiofrequency. For imaging purposes, the external static magnetic field has to be varied locally (spatial encoding) to allow the formation of a two-dimensional image from the acquired signal. From stacks of parallel images, three-dimensional information can be obtained. For clinical use of MRI, magnetic field strengths are typically around 1 Tesla, created by large superconductive coils in which the subject is placed.

The aim of the present study was to investigate in humans the intragastric distribution of a colloidal drug carrier (Gd-DOTA-labeled liposomes) released from hard gelatin capsules after ingestion of either a liquid or a mixed solid-liquid meal using MRI.

MATERIALS AND METHODS

Preparation of Gadolinium-DOTA-Liposomes

An ethanolic solution of 4.5 g soya phosphatidylcholine (Lipoid S-PC, Lipoid AG, Cham, Switzerland) was placed into a round bottom flask. The solvent was removed by rotary evaporation under reduced pressure at 40°C. The lipid film obtained was hydrated for 60 min in 30 ml of a gadolinium-DOTA (Gd-DOTA) solution (gadolinium tetraazacyclododecane tetraacetic acid, Dotarem, Laboratoire Guerbet, Aulnay-sous Bois, France). The resulting dispersion was extruded through polycarbonate filters (400, 200, and 100 nm pore size, Satorius membare filter device, Göttingen, Germany) under nitrogen pressure and dialysed against 0.9% sodium chloride solution for 2 hours using a Lipoprep-GD-1 instrument (Diachema AG, Rüschlikon, Switzerland). Dispersions were centrifuged in a Beckman TL-100 ultracentrifuge at 100,000 g for 30 min. (Beckman Instruments International, Basel, Switzerland). Approximately ⅔ of the clear supernatant in the tubes were removed, the remaining content was pooled and vortexed. The liposomal dispersions were stored at 4°C for no longer than 48 h before being used in the study.

Characterization of Gd-DOTA-Liposomes

Hydrodynamic radii and polydispersity of the liposomal dispersion were 157 ± 2 nm (n = 6), and polydispersity index (PI) = 2-3 (Nano sizer PSM 78, Coulter Electronics, Krefeld, Germany; PI ranging from 0 = homogenous to 9 = heterogeneous). The gadolinium concentration in the dispersion was

[1] Biophysics group, Institute of Biomedical Engineering and Medical Informatics, University and ETH Zurich, Switzerland.
[2] Department of Gastroenterology, University Hospital Zurich, Switzerland.
[3] F. Hoffmann-La Roche, PRPI/PRNF, Basel, Switzerland.
[4] To whom correspondence should be addressed. (e-mail: gasschwi@usz.unizh.ch)

0724-8741/01/0400-0460$19.50/0

determined by energy-dispersive x-ray fluorescence (EDXRF, Spectro X-Lab, Spectro GmbH, Cleve, Germany) and was found to be 0.90%.

Stability of Gd-DOTA-Liposomes

In preliminary experiments using EDXRF, it was found that more than 97% of the Gd-DOTA remained encapsulated in the liposomes for 2 days of storage at 4°C. Incubating the liposomal dispersion for 2 hours in human gastric juice (Department of Gastroenterology, Kantonsspital Basel, Switzerland, pH 4.5), aqueous 20% glucose solution or a 1:1 v/v mixture of human gastric juice and glucose solution at 37°C did not lead to a change in the average size of the liposomes (153-158 nm, PI = 2-3). More than 85% of Gd-DOTA remained encapsulated in the liposomes after 2 hours of incubation (determined by EDXRF after ultracentrifugation of the dispersions). The density of the liposomal dispersion at 37°C was determined to be 1.02, the density of the 20% glucose solution was 1.07.

Preparation of Hard Gelatin Capsules Containing Gd-DOTA-Liposomes

Empty hard gelatin capsules (size 0) were band-sealed using a 5% w/w solution of hydroxypropylmethylcellulose-acetate-succinate (HPMCAS) in a 1:1 v/v mixture of ethanol and acetone. 670 μl of the liposomal dispersion was injected into the transparent, closed, sealed capsules. After sealing of the injection hole with HPMCAS solution and allowing it to dry for 1 min, the capsule was immediately given to the subjects positioned in the MR imager.

Subjects

Eight healthy subjects (7 male, 1 female) between 21 and 27 years participated in the study. The subjects were not taking any medication prior to or during the study and had no history of gastrointestinal disease. Written informed consent was obtained, and the protocol was approved by the ethics committee of the University Hospital Zurich.

MR Imaging Technique

The MRI investigations were performed with a commercial 1.5 Tesla whole body imager (Gyroscan ACS-NT, Philips Medical Systems, Best, NL). After the subjects were positioned in the MRI instrument, sets of 20 parallel images of the gastric region were acquired at regular time intervals. The time required for a complete image set was 20 s. The resolution in three dimensions was given by the in-plane resolution of the 2D images and the slice thickness, that is 1.7 * 1.7 * 8 $mm.^3$ In each image, the outline of gastric content was then determined in a semiautomatic procedure based on the anatomical structures visible in the images. This yielded all volume elements ('voxels') within the stomach content, which were then differentiated according to their signal intensity.

The contrast agent leads to a local increase in signal intensity by affecting the protons in its vicinity. To differentiate between regions in the stomach containing Gd-DOTA and regions in the stomach which do not contain the contrast agent (background), a threshold signal intensity was chosen. To achieve this, the intensity distribution of the voxels within the stomach content after the capsule has been given was determined and compared with the intensity distribution of the voxels within the stomach content of a scan taken prior to the administration of the capsule (reference scan). Each voxel with an intensity above the highest intensity in the reference scan was assumed to be a volume element of the stomach containing Gd-DOTA. To standardize the image intensity between images and over the course of the study, all images were referenced to the signal intensity of the liver and an external reference as control. In order to determine the distribution of high concentrations of the contrast agent, a second threshold ("high threshold") 25% above the highest intensity in the reference scan was chosen. Since the image information is purely one of intensity, care has to be taken to ensure that contributions from the desired compound are clearly distinct in intensity from the surrounding. To achieve this, a wide variety of techniques is available (see discussion). To avoid interference of the intense signal from the protons of fatty acid chains (i.e., from body fat or ingested fat) with the Gd-DOTA signal, the contributions from fat were suppressed by selective excitation and subsequent dephasing of the undesired signal prior to imaging.

To follow the distribution of the fat component of the meal, the ingested fat component was selectively imaged in separate scans ('fat scan') by suppression of the water signal, as described above.

The MR data set of 20 parallel, transverse slices was also reformatted to a coronal view, to allow a better appreciation of the local variations in the distribution process.

A *maximum intensity projection* was calculated to obtain a two-dimensional visual impression of the distribution. In this projection, the observer is assumed to be looking from a fixed direction onto the three-dimensional image stack (in our study, the z direction along the scanner axis). To compress this 3D information (x,y,z) to a 2D image, the intensity of each point (x,y) of the maximum intensity projection image is determined by the highest intensity of the voxels at the same (x,y) position in any of the 20 slices. The total of all voxels corresponds to the intragastric content at each time point. From this, the percent decrease of gastric content was calculated. Gastric emptying was expressed as the percentage of gastric content remaining after 90 min (9).

All calculations were done for the whole stomach and for antrum and fundus. to obtain antral and fundic sub-regions, the stomach was devided at the angula, as identified from three-dimensional reconstructions of the stomach.

Study Protocol

Subjects were allowed a light breakfast before 8:00 a.m., but no food or drinks except water thereafter, and arrived at the unit in the early afternoon. Each subject was studied on two occasions. After ingestion of either a liquid or a solid meal, subjects were positioned in the MR imager lying with the left side elevated at an angle of 30° to the horizontal. A reference scan was performed to map the signal intensity of gastric content. Then, a hard gelatin capsule filled with an aqueous dispersion of liposomally encapsulated Gd-DOTA as MR contrast agent (10) was ingested. Opening of the capsule and the dynamic distribution of the liposomes was followed over 90 min. MRI scans were performed continuously until release of the colloidal dispersion from the capsule was

first observed (t = 0 min), thereafter every 2 min until t = 20 min, then every 5 min until t = 50 min and finally every 10 min until t = 90 min. To trace the distribution of the fat phase of the solid meal, an image of the fat signal was obtained prior to capsule administration, at t = 20 min and thereafter every 15 min until the end of the study. In one subject, opening of the capsule occurred prior to the first scan. The data from this subject were therefore excluded from the analysis.

Test Meals

500 ml 20% glucose solution (400 kcal) served as liquid meal. The solid meal (645 g) consisted of a fat-free component (270 g spaghetti, 200 g fat-free tomato sauce) and a fat component (40 g mayonnaise on 35 g toast) and was served together with 100 ml water. The fat component was ingested after the first half of the fat-free meal component. The energy content of the meal was 795 kcal with 53 energy percent from carbohydrates, 10 energy percent from protein and 37 energy percent from fat. The liquid content of the meal was 30%.

Determination of Maximum Distribution Volume

To compare the maximum distribution volume of liposomes with the distribution volume of an aqueous solution, the liposomal content of the ingested capsule was replaced by a Gd-DOTA solution in a pilot experiment. For this purpose, five subjects ingested a hard gelatin capsule containing 670 μl Gd-DOTA solution after ingestion of the solid meal. The distribution of the contrast agent was then traced over 60 min and the maximum distribution volume of the Gd-DOTA solution was found to be 29 ± 2%.

Statistical Analysis

Data are expressed as means ± SEM. A paired, two-tailed t-test and a Wilcoxon rank sum test were used to test for statistical significance. $P < 0.05$ was regarded as statistically significant.

RESULTS

Liquid Meal

Distribution of the liposomes could be followed in all subjects and all time periods. Capsule opening occurred in the fundus on the surface of the liquid meal. On release from the capsule in the fundus (2.5 ± 0.6 min after ingestion), its liposomal content rapidly formed a layer on the liquid surface (Figures 1, 2b).

Figure 2 shows the characteristics of the liposomal distribution in a maximum intensity projection and in the intensity histograms. Immediately after capsule opening, the layer of Gd-DOTA liposomes (Figure 2b) occupied only a small fraction of the total meal volume (11 ± 4% at 2 min after capsule opening), while the single peak in the histogram (Figure 2a) represented the background intensity of the part of the meal that had not mixed with the liposomes. After this initial period, liposomes covered a larger proportion of the total liquid volume, resulting in a second peak in the histogram at higher intensities (Figure 2a). At 80 min, the difference between background intensity and liposomes in the histogram had disappeared as shown in the maximum intensity

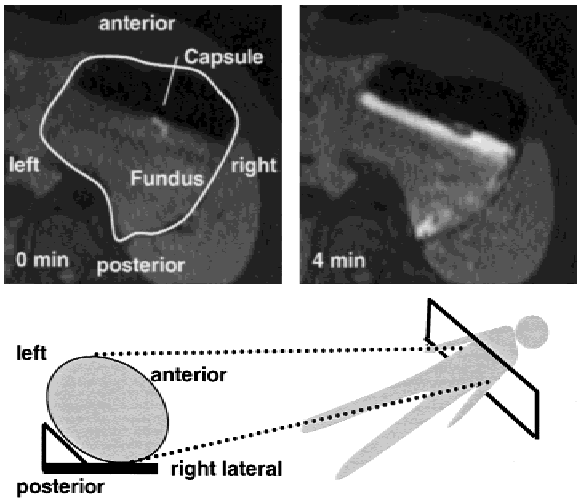

Fig. 1. MR images (view from feet to head) at two time points showing distribution of the liposomes in the fundus after ingestion of a liquid meal. Subjects were lying with the left side elevated at an angle of 30° to the horizontal. Following release from the capsule, Gd-DOTA filled liposomes provided a high signal intensity in the images.

projection (Figure 2b), indicating a homogenous distribution of liposomes in the liquid meal. After 90 min, 38 ± 11% of the initial volume was still present in the stomach.

Distribution of the liposomes in the entire meal volume reached a maximum (86 ± 2% of total volume, corrected for gastric emptying) at 42 ± 6 min (Figure 3a). To assess the inhomogeneity of the liposomal distribution, a second high-threshold (25% above the lower) was chosen to identify voxels with a higher concentration of liposomes. This high threshold revealed that distribution of higher concentrations of liposomes occurred faster in the fundus than in the antrum until 40 min ($P < 0.05$, Figure 3b), resulting in an early distribution of liposomes in the fundus. Liposome distribution into the antrum was slow until 20 min after capsule opening (antral distribution volume increasing by 6 ± 3% per 10 min). After that time, distribution into the antrum was faster (antral distribution volume increasing by 31 ± 10% per 10 min, $P < 0.05$) until maximum distribution was reached. Thereafter, no difference was found between the two gastric regions.

Solid Meal

The liposomal preparation and the fat component could be visualized in the solid meal in all subjects (Figure 4). Figure 5 shows a maximum intensity projection of the liposomal distribution in the solid meal. Capsule opening (3.0 ± 0.7 min after capsule intake) occurred in the fundus, where a high liposome concentration was observed in all subjects around the gastro-esophageal junction. The site, where liposomes were concentrated, remained stationary throughout the study period (Figure 5b). In contrast to the liquid meal, no layering was observed. Distribution of the liposomes was confined to a small volume, which is shown by the fact that no prominent 'liposomal' peak was found in the histograms (Figure 5a) and that the intensity of the meal (the maximum of the main peak in the histogram in Figure 5a) was not shifted towards higher intensities. After 90 min, 67 ± 5% of the initial volume was still present in the stomach.

Maximum distribution of the liposomes in the entire

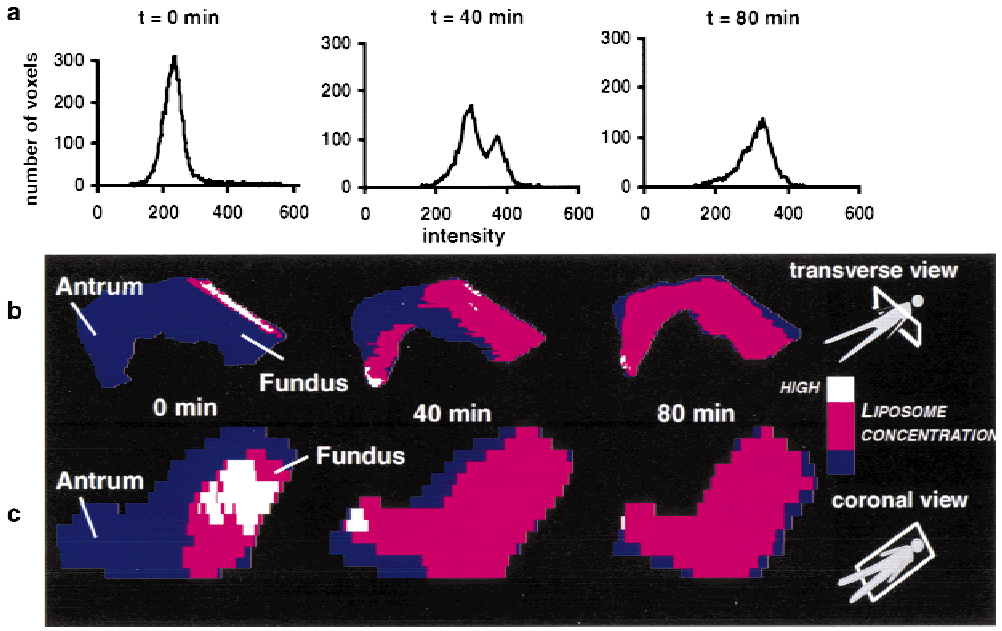

Fig. 2. (a) Intensity histograms showing the distribution of the liposomes (high intensities) in the meal at three different time points. At intermediate time intervals (40 min), two close but distinct peaks appeared, which eventually merged and resulted in a single peak (80 min) indicating homogeneous distribution. (b) Maximum intensity projection of the liposome distribution (bright colours) in transverse and (c) coronal views: at t = 0 min, opening of the capsule floating on the surface of the liquid (dark blue) and initial rapid layering of the liposomes on the surface (white) was observed, followed by distribution first in the fundus and finally, a near-homogeneous distribution.

meal volume was reached after 24 ± 6 min, faster than with the liquid meal ($P < 0.05$). The liposome distribution reached a plateau of constant distribution volume (1% of the maximum value) between 12 ± 2 min and 33 ± 8 min. Maximum distribution volume (obtained with the low threshold) was much lower (7 ± 1%) compared with the liquid meal ($P < 0.05$; Figure 6) and the Gd-DOTA solution in the solid meal (29 ± 2%, see methods).

Fat Distribution

In all subjects, the distribution of the dietary fat could be clearly identified. Fat distribution was highly inhomogeneous, as shown in the maximum intensity projection plots (Figure 5c). The largest part of the fat was located close to the surface forming a distinct region at a site different from that of the liposomes over the entire 90 min.

DISCUSSION

In this study, we have developed a technique to monitor in humans the intragastric passage of a colloidal drug carrier model (Gd-DOTA-labeled liposomes). The technique was then applied to identify major mechanisms and characteristics of the distribution process that are of importance for designing oral delivery forms.

The advantages of MRI for studies of this nature are that 3D information is available not only on the drug delivery system and selected food components, but also of the surrounding anatomy. This allows a more specific interpretation of the data in different areas of the gastrointestinal tract and combination with other functional tests such as the assessment of gastric emptying, as shown in this study. In recent

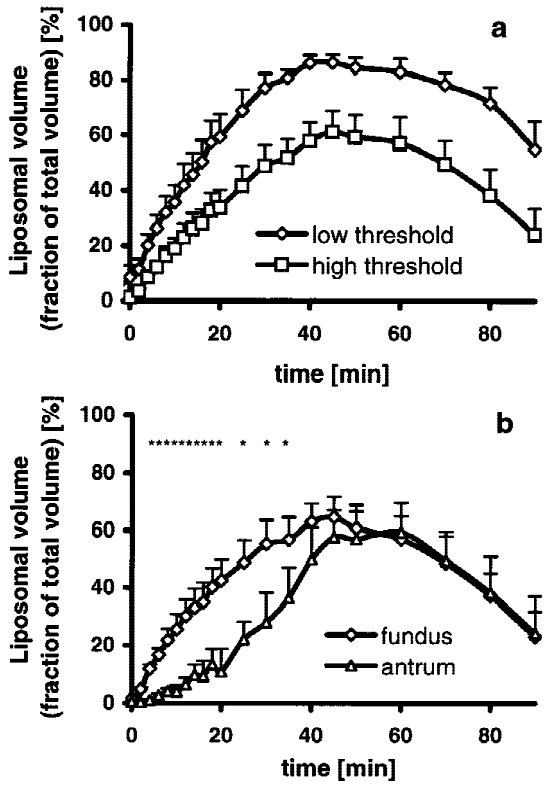

Fig. 3. (a) Kinetics of distribution of the colloidal system in the liquid meal at two detection thresholds (high and low). (b) Distribution of higher liposome concentrations (high detection threshold) occurred faster in the fundus than in the antrum until 40 min. Thereafter, no difference was found between the two gastric regions. Asterisks indicate significant difference between distributions at each time point.

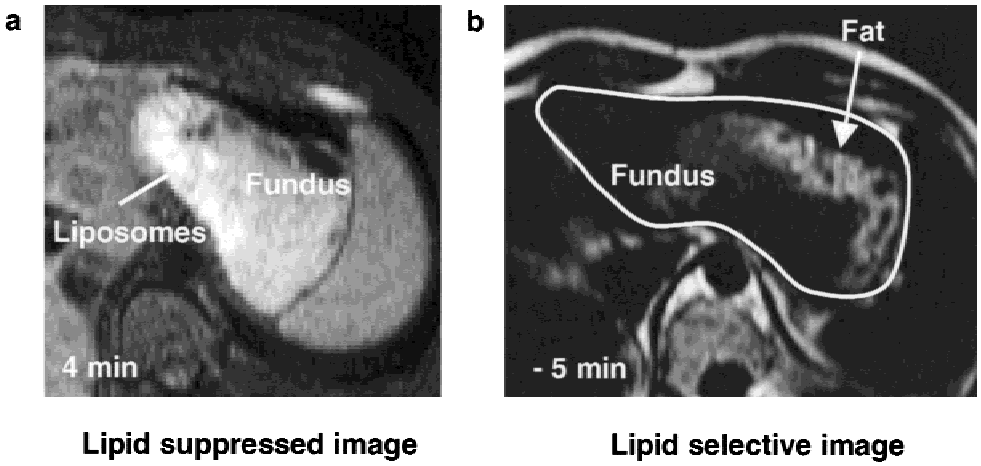

Fig. 4. MR image showing the distribution of the colloidal drug carrier (a) and dietary fat (b, before capsule intake) in the fundus after ingestion of the solid meal.

years, MRI has become a versatile, established research tool for the study of gastric motor function (9,11,13–17).

A drawback of the technique presented here lies in the way the delivery system is labeled. MRI contrast agents such as gadolinium can, for safety reasons, not easily be chemically linked to the drugs themselves. Moreover the complexation of gadolinium with a drug would alter the physico-chemical properties of the drug. A simple alternative is to use 'natural' contrast mechanisms, e.g. between lipids and water, where the fatty acid chain protons themselves provide a detectable signal. The approach taken in the present study to overcome this difficulty was to label a model delivery system with desired properties and enclosing the contrast agent therein. We used liposomes as a colloidal drug delivery system, being aware of the fact that they cannot be regarded as an ideal oral delivery system because of their physical instability in the lower GI tract, especially if they come in contact with bile salts in the small intestine. However, the *in vitro* experiments using human gastric juice indicated that leakage of the hydrophilic contrast agent from the liposomes in the stomach over 90 minutes was small. This interpretation is further supported by the difference found between the maximum volume distribution of the Gd-DOTA solution and GD-DOTA containing liposomes in the solid meal. While the arguments given above are not entirely confirmatory, it is reasonable to believe that, for the study on intragastric behavior, liposomes do represent a suitable model for a colloidal system with particle sizes of around 150 nm.

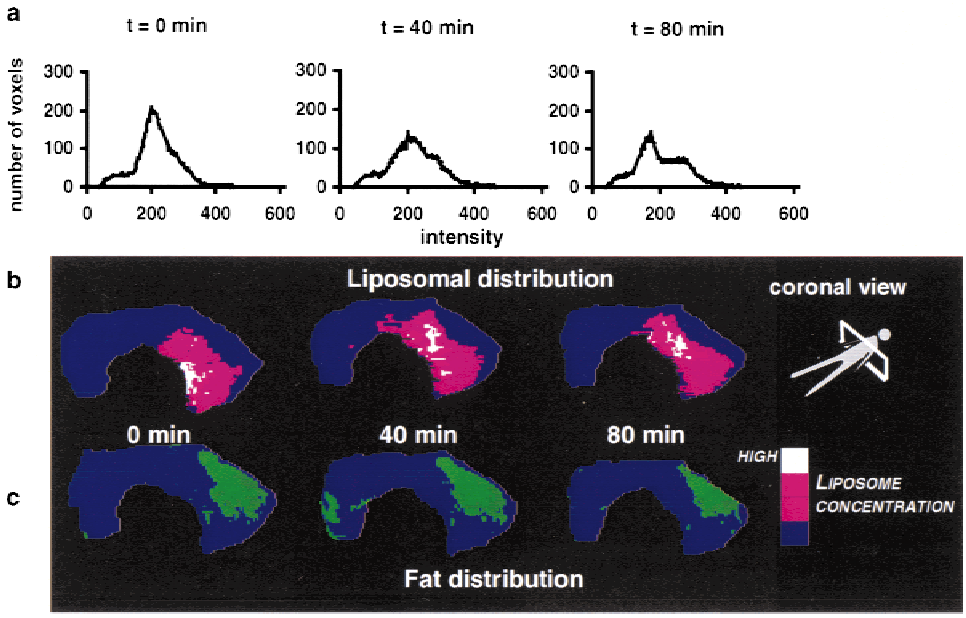

Fig. 5. Intragastric distribution of liposomes containing Gd-DOTA after ingestion of the solid meal. (a) The histograms show no distinct signal peak attributable to the colloidal system indicating confinement to a small volume. (b) Maximum intensity projection of the liposome distribution in transverse view. A 'hot spot' with a high concentration of liposomes in the fundus remained stationary over the study period. (c) Maximum intensity projection of the fat distribution. The largest part of the fat was located at a site different from the liposomal 'hot spot'.

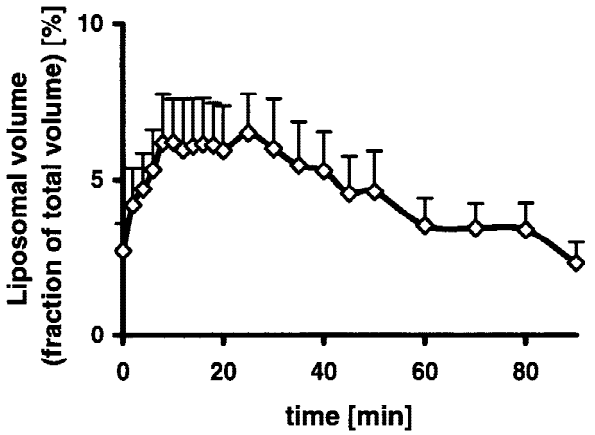

Fig. 6. Kinetics of the liposomal distribution in the solid meal. Distribution of the liposomes was confined to a small volume.

From a practical viewpoint, this technique has the important advantage of not requiring dedicated hardware, thus being readily transferable to standard clinical MR imagers. Furthermore, we used a standard MR contrast agent, Gd-DOTA, that is not absorbed in the GI tract (13). Applicability of MRI to track delivery systems is limited by the fact that all contrast agents currently approved for clinical use are hydrophilic. Lipophilic contrast agents would greatly extend the range of drug delivery systems that can be studied by MRI. A lipophilic marker could be included into micellar systems, o/w-microemulsions, submicron emulsions, solid lipid nanoparticles, self-emulsifying systems, amongst others. While such novel contrast agents are under development (12), these can not be expected to be available in the near future.

An alternative approach for using MRI to monitor drug delivery systems is the use of double contrast techniques. With this technique, a nucleus other than ^{1}H, but which also yields an NMR signal, is imaged. For example, ^{19}F can be used as a specific tracer in contrast to ^{1}H. In one study, the fluorine content of an intact capsule was visualized by imaging ^{19}F overlaid on the standard water (^{1}H) MR image (18). A similar technique was used to investigate the behavior of solid oral dosage forms (microtablets and minicapsules) in the gastrointestinal tract of rats (19). This method offers high selectivity for the drug model against background 'noise' (e.g., the meal and surrounding viscera) at the cost of lower sensitivity to the delivery system compared with ^{1}H imaging.

The present study in humans demonstrates that the intragastric distribution of the colloidal drug carrier model depends substantially on the physicochemical characteristics of the meals. In the liquid meal, distribution was characterized by initial layering (explained by the density difference between the liquid meal and the colloidal dispersion), and a near homogenous distribution of the drug model within about 40 min. While diffusion can be ruled out as a factor, convection was most likely responsible for the distribution of the colloidal system in the liquid meal. Dilution of the liposomal Gd-DOTA concentration by gastric secretion, leading to a reduction in signal intensity, is likely to be responsible for the decrease in distribution volume after the maximum had been reached. Distribution of the drug model after ingestion of the solid meal was confined to a small volume, indicating that substantial parts of gastric content were not accessible to the colloidal system. This must be taken into account when a steady delivery of chyme mixed homogeneously with the drug to the small intestine is important for the efficacy of a drug.

Additional information with possible consequences for designing drug delivery systems can be drawn from monitoring individual food components. We observed that the fat contained in the meal did not distribute homogeneously within the solid phase, but remained largely stationary throughout the study period. A spatial separation between the sites of the fat and the drug model persisted over the course of the study period, demonstrating that drugs in the stomach are not necessarily well mixed with dietary fat. The distribution of a drug carrier especially in relation to the fat components of a meal may have substantial consequences for the bioavailability of drugs (3). For example, intraluminally acting enzymes affecting fat digestion in chronic pancreatic insufficiency or cystic fibrosis, rely on the simultaneous arrival of enzymes and fat in the small intestine (20).

In summary, this study has shown that MRI monitoring of oral dosage forms offers important information on the distribution process for the optimization of new drug delivery systems and could complement insight gained by other imaging techniques.

ACKNOWLEDGMENTS

The study was supported by the Swiss National Science Foundation (SNF grants: 32-54056.98 and 31-55932.98).

REFERENCES

1. H. A. May, C. G. Wilson, and J. G. Hardy. Monitoring radiolabeled antacid preparations in the stomach. *Int. J. Pharm.* **19**:169–176 (1984).
2. N. Rouge, P. Buri, and E. Doelker. Drug absorption sites in the gastrointestinal tract and dosage forms for site-specific delivery. *Int. J. Pharm.* **136**:117–139 (1996).
3. W. N. Charman, C. J. H. Porter, S. Mithani, and J. B. Dressman. Physicochemical and physiological mechanisms for the effects of food on drug absorption: The role of lipids and pH. *J. Pharm. Sci.* **86**:269–282 (1997).
4. M. J. Bruno, E. B. Haverkort, G. N. J. Tytgat, and D. J. Van Leeuwen. Maldigestion associated with exocrine pancreatic insuffiency: Implications of gastrointestinal physiology and properties of enzyme preparations for a cause-related and patient-tailored treatment. *Am. J. Gastroenterol.* **90**:1383–1393 (1995).
5. S. S. Davies, J. G. Hardy, S. P. Newmann, and I. R. Wilding. Gamma scintigraphy in the evaluation of pharmaceutical dosage forms. *Eur. J. Nucl. Med.* **19**:97–986 (1992).
6. C. G. Wilson and N. Washington. Assessment of disintegration and dissolution of dosage forms in vivo using gamma scintigraphy. *Drug. Dev. Ind. Pharm.* **14**:211–281 (1988).
7. I. R. Wilding, A. J. Coupe, and S. S. Davies. The role of gamma scintigraphy in oral drug delivery. *Adv. Drug. Deliver. Rev.* **7**:87–117 (1991).
8. C. G. Wilson, M. McJury, B. O'Mahony, M. Frier, and A. C. Perkins. Imaging oily formulations in the gastrointestinal tract. *Adv. Drug Deliver. Rev.* **25**:91–101 (1997).
9. P. Kunz, G. R. Crelier, W. Schwizer, J. Borovicka, C. Kreiss, M. Fried, and P. Boesiger. Gastric emptying and motility: Assessment with MR imaging—Preliminary observations. *Radiology* **207**:33–40 (1998).
10. C. Tilcock, E. Unger, P. Cullis, and P. MacDougall. Liposomal Gd-DTPA: Preparation and characterisation of relaxivity. *Radiology* **171**:77–80 (1989).
11. C. Feinle, P. Kunz, P. Boesiger, M. Fried, and W. Schwizer. Scintigraphic validation of a magnetic resonance imaging technique to study gastric emptying in humans. *Gut* **44**:106–111 (1999).

12. G. W. Kabalka, M. A. Davis, T. H. Moss, E. Bounocore, K. Hubner, E. Holmberg, K. Maruyama, and L Huang. Gadolinium labeled liposomes containing various amphiphilic Gd–DTPA derivatives: Targeted MRI contrast enhancement agents for the liver. *Magn. Reson. Med.* **19**:406–415(1991).
13. W. Schwizer, M. Fried, and H. Maecke. Measurement of gastric emptying in humans by magnetic resonance imaging. *Gastroenterology* **103**:369–376 (1992).
14. W. Schwizer, R. Fraser, J. Borovicka, K. Asal, G. Crelier, P. Kunz, P. Boesiger, and M. Fried. Measurement of proximal and distal gastric motility with magnetic resonance imaging. *Am. J. Physiol.* **271**:G217–G222 (1996).
15. P. Boulby, P. Gowland, V. Adams, and R. C. Spiller. Use of echo planar imaging to demonstrate the effect of posture on the intragastric distribution and emptying of an oil/water meal. *Neurogastroenterol. Motil.* **9**:41–47 (1997).
16. P. Boulby, R. Moore, P. Gowland, and R. C. Spiller. Fat delays emptying but increases forward and backward antral flow as assessed by flow-sensitive magnetic resonance imaging. *Neurogastroenterol. Motil.* **11**:27–36 (1999).
17. D. A. Adkin, P. Gowland, R. C. Spiller, A. Freeman, J. Hykin, B. Issa, P. D. Huckle, and I. R. Wilding. Echo-planar magnetic resonance imaging to assess water volume in the distal small bowel. *Pharm. Res.* **12**:1134–1139 (1995).
18. R. Schwarz, M. Schuurmans, J. Seelig, and B. Kuennecke. ^{19}F-MRI of perfluoronanane as a novel contrast modality for gastrointestinal imaging. *Magn. Reson. Med.* **41**:80–86 (1999).
19. V. Christmann, J. Rosenberg, J. Seega, and C. M. Lehr. Simultaneous in vivo visualisation and localisation of solid oral dosage forms in the rat gastrointestinal tract by magnetic resonance imaging (MRI). *Pharm. Res*. **14**:1066–1072 (1998).
20. M. Fried. Chronic pancreatitis: treatment of pancreatic insufficiency and pain. In M. W. Büchler, W. Uhl, H. Friess, P. Malfertheiner (eds.), *Acute Pancreatitis: Novel concepts in biology and therapy*, Blackwell Wissenschafts-Verlag, Berlin, 1999 pp. 509–512.